Stability of Unstructured Block Ramps

Volker Weitbrecht[1]; Simona Tamagni[2]; and Robert M. Boes[3]

Abstract: Unstructured block ramps fish-friendly structures to stabilize a riverbed, characterized by large macroroughness elements randomly placed on the riverbed. Physical model tests were conducted to investigate their stability and their behavior in case of overload. Different parameters describing the block and the base material were tested to find an optimal combination in terms of ramp stability with a maximum ramp slope typically in the range of 1–3%. A model for the determination of the ramp stability is presented, where the equilibrium slope of the ramp is related to a dimensionless specific discharge including information on the block size, the block placement density, and a characteristic grain size of the base material. **DOI: 10.1061/(ASCE)HY.1943-7900.0001259.**

Author keywords: Unstructured block ramps; Physical experiments; Fish migration; Riverbed stability.

Introduction

Worldwide rivers are interrupted by drops and sills or other artificial structures precluding upstream migration of fishes and other animals. In Switzerland, approximately 100,000 such structures exist with an elevation difference larger than 0.5 m (Zeh Weissman et al. 2009). This situation led to fragmented habitat conditions and to strongly reduced abundance of the pristine fish fauna (Werth et al. 2011; Alp et al. 2011). To improve the situation on a larger scale, drops and sills need to be replaced so that (1) riverbed stability and (2) habitat connectivity are guaranteed. A compromise regarding aspects of riverbed stability and fish migration is given by the use of ramps to overcome a certain height difference as illustrated in Fig. 1. In the case of a ramp, the kinetic energy is dissipated over a certain length and not as in the case of a drop at a single location, leading to improved fish migration. During the last decades many existing drops have been replaced by block ramps and many more are planned. However, during the 2005 flood and other flood events in Switzerland many block ramps failed (e.g., Bezzola and Hegg 2008), showing that existing design criteria are insufficient and the stability is often overestimated. The need of sustainable river restoration measures and of uninterrupted longitudinal connectivity of watercourses makes the present research significant to Alpine regions.

The present paper summarizes Phase A of an extensive set of physical experiments as part of a Ph.D. project (Tamagni 2013) performed at the Laboratory of Hydraulics, Hydrology, and Glaciology (VAW) with special focus on the structural stability and the application range of unstructured block ramps (UBR). Phase B on turbulence aspects (Tamagni et al. 2014) and Phase C on the general behavior of UBR (Tamagni 2013) are not discussed in this paper. A stability criterion is presented to relate a certain specific discharge to a maximum bed slope of the ramp allowing for a straightforward predesign of bed slope, block diameter, and block placement density. In addition, the approach of Pagliara and Chiavaccini (2006) to describe the flow resistance on reinforced block ramps is adapted to better describe the flow on UBR.

Design and Hydraulic Characteristics of Block Ramps

Classification

According to the classification given in Fig. 2, block ramps are divided into two groups. The block carpet type includes the classic block ramp design, involving tightly packed blocks or riprap that form a block carpet covering the entire river width. They can be subdivided into interlocked block ramps characterized by one layer of blocks vertically placed closely together, leading to a compact, hydraulically solid but rigid construction; and dumped block ramps where the blocks are randomly dumped in two or more layers, leading to a heavier and more heterogeneous construction. Experience shows that these ramps should not be used for bed slopes larger than 10% (Hunziker, Zarn & Partner 2008).

Ramps of the block cluster type are characterized by different dispersed configurations of block clusters, leading to more natural conditions due to their distinctive heterogeneity. In the case of structured geometrical configuration of the blocks, e.g., rows or arches generating a step-pool system, they are called structured block ramps, corresponding to the characteristic morphology of mountain rivers. During low and medium discharge, these sequences of pools and steps offer more suitable hydraulic conditions for fish migration compared to the block carpet type. According to LUBW (2006) the maximal slope for structured block ramps is about 7%. In the case of self-structured block ramps the idea is that the energy dissipating step-pool system develops during high discharge conditions. To achieve suitable conditions for the self-structuring process, the riverbed is replenished with coarse bed

[1]Head, River Engineering Division, Laboratory of Hydraulics, Hydrology and Glaciology (VAW), Swiss Federal Institute of Technology, ETH Zurich, 8093 Zürich, Switzerland (corresponding author). E-mail: weitbrecht@vaw.baug.ethz.ch

[2]Research Engineer, Beffa Tognacca GmbH, 6702 Claro, Switzerland; formerly, Laboratory of Hydraulics, Hydrology, and Glaciology (VAW), Swiss Federal Institute of Technology, ETH Zurich, 8093 Zürich, Switzerland. E-mail: stamagni@fluvial.ch

[3]Professor and Director of VAW, Laboratory of Hydraulics, Hydrology and Glaciology (VAW), Swiss Federal Institute of Technology, ETH Zurich, 8093 Zürich, Switzerland. E-mail: boes@vaw.baug.ethz.ch

Note. This manuscript was submitted on February 1, 2016; approved on August 9, 2016; published online on October 27, 2016. Discussion period open until March 27, 2017; separate discussions must be submitted for individual papers. This paper is part of the ***Journal of Hydraulic Engineering***, © ASCE, ISSN 0733-9429.

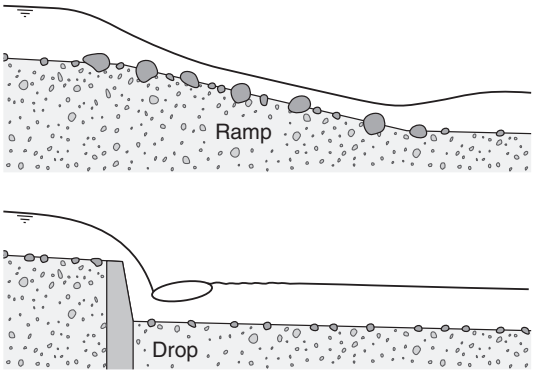

Fig. 1. Ramp versus drop; energy dissipation on the ramp occurs on longer section compared to a drop structure, improving upstream migration for certain fish species

Fig. 3. Upstream view of UBR at the Landquart River, Switzerland, with specific discharge $q \approx 0.28$ m^2/s (image by authors)

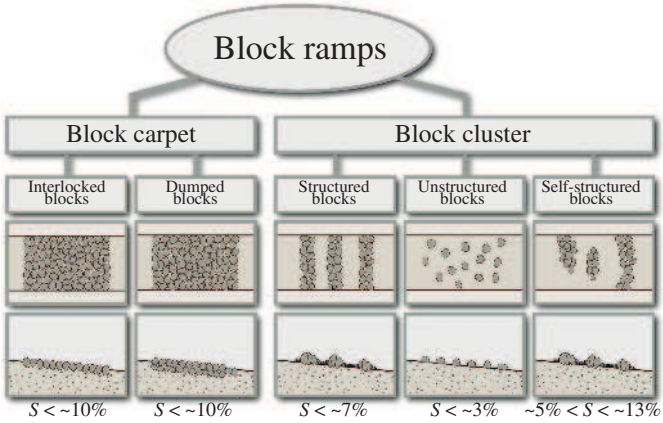

Fig. 2. Classification of block ramps (adapted from Lange 2007)

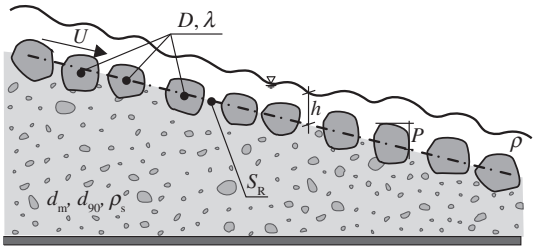

Fig. 4. Longitudinal section of an UBR with the most important parameters: U = bulk flow velocity; h = water depth; P = protrusion of a block above the gravel bed; λ = block placement density; D = block diameter (equivalent diameter of a sphere with the same mass); d_m = mean grain size of the bed material; d_{90} = grain size of the bed material with 90% sieve passing; ρ_s = sediment density; ρ_w = water density; and S_R = bed slope

material and blocks. According to Lange (2007) and Weichert (2006) the bed slope of self-structured block ramps ranges from 5 to 13%.

The focus of the present paper is on UBR (Figs. 2 and 3), a third variation of the block cluster type of ramps. In the case of UBR, large blocks are randomly placed on the riverbed with a certain block placement density λ, defined as the ratio between the area covered by blocks and the total ramp area [Eq. (2)]. There is neither contact between the boulders nor a geometrical regular block configuration. The randomness of the block positions leads to a strong geometrical and flow field heterogeneity, resulting in efficient energy dissipation and offering a large variety of migration corridors for different fish species and their specific swimming capacity. According to Janisch (2007) the maximal slope of UBR is 3%. Fig. 3 shows an example of an UBR at the Landquart River with a width of approximately 20 m and a slope of 2% that has been realized within a series of ramps from 2008 to 2012. A list of different UBR built in Switzerland can be found in the appendix of Tamagni (2013).

Flow Resistance and Equilibrium Slope

No universally valid approach to characterize flow and ecological conditions on block ramps is available, especially for UBR, due to the complexity of the flow processes (DWA 2009; Tamagni et al. 2014). Therefore, the design of new block ramps as well as the prediction of their stability and of their ecological effectiveness is still limited. The flow depth h and the mean flow velocity U constitute the fundamentals for the hydraulic design of block ramps (Fig. 4). However, the variation of the block configuration and thus of the roughness on the ramp in both longitudinal and transverse directions leads to highly heterogeneous flow conditions and hence to strong local variations of h and U.

Pagliara and Chiavaccini (2006) determined the influence of large blocks on the flow resistance by testing reinforced block ramps with protruding boulders placed in rows or randomly distributed, which can be defined as structured and unstructured block ramps of block cluster type, respectively. The blocks were placed and glued on a fixed layer of bed material (4 mm < d_{84} < 24.7 mm) made of rounded or crushed rocks with an almost uniform granulometric curve [$1.05 < \sigma = (d_{84}/d_{16})^{0.5} < 1.26$]. Local block movements or entrainment and erosion processes of the bed material is prevented in the study of Pagliara and Chiavaccini (2006). Their experiments resulted in the following equation of flow resistance for reinforced ramps

$$\frac{U}{u_*} = \frac{U}{\sqrt{ghS}} = 3.5(1+\lambda)^C S^{-0.17}\left(\frac{h}{d_{84}}\right)^{0.1} \quad (1)$$

where C = coefficient describing the base material and the block arrangement; U = bulk streamwise velocity; u_* = shear velocity; g = gravity acceleration; S = ramp slope; d_{84} = characteristic grain

diameter of the bed material; and λ = block placement density defined as

$$\lambda = \frac{N\pi D^2}{4W_R L_R} \tag{2}$$

where N = number of blocks along the entire ramp; D = equivalent spherical block diameter; W_R = ramp width; and L_R = ramp length. Eq. (1) is valid for the tested parameter range, with $8\% < S < 40\%$, $1.9 < D/d_{50} < 14.5$, $0 < \lambda < 0.3$, relative submergence levels $0.2 < h/P < 2.6$ (here P = block protrusion = $D/2$), Reynolds number $1.5 \times 10^4 < \mathrm{R} = UR/\nu < 20 \times 10^4$ with R = hydraulic radius and ν = kinematic viscosity and Froude number $0.8 < \mathrm{F} = U/(gh)^{0.5} < 2.2$. Eq. (1) shows that the flow resistance is related to S, the block arrangement (blocks in rows are more dissipative than blocks in random disposition) and particularly on λ, while the influence of h/P, F, and R appears negligible for the tested parameter range. The aim of this research is to extend the application range of the existing approach by investigating ramps with similar conditions as in the prototype, e.g., using natural blocks and testing the ramps without fixing the bed material.

Stability and Design Requirements of UBR

Compared to block carpet type ramps and to drops and sills, UBR offer two advantages, namely (1) improved fish migration, and (2) gradual failure in case of discharge overload, due to the flexibility of the structure that prevents an abrupt failure. During flood events UBR can adjust themselves to the higher discharge through erosion and sorting processes leading to a decreased bottom slope. According to Raudkivi and Ettema (1982) the bimodal mixture of sediment on a UBR, consisting of large blocks and finer bed material, implies two dominant failure mechanisms: (1) overpassing of the blocks, and (2) embedding of the blocks into the finer bed material. To avoid these the ratio between the block diameter D and the characteristic grain size of the bed material d has to follow $6 < D/d < 17$. For bed material with a wide grain size distribution where an armoring layer can develop (as in the case of typical Alpine conditions) the characteristic grain size of the bed material is d_{90} (Janisch et al. 2007).

For the design of UBR, two main criteria must be fulfilled, namely a (1) hydraulic, and (2) ecological criterion. For (1) the structural integrity of the block ramp has to be ensured up to a certain design discharge that usually corresponds to the 100-year flood $\mathrm{H}Q_{100}$; as to (2) block ramps have to be ecologically effective in a certain range of discharges related to the hydrology of a river (DWA 2009). In Switzerland it is assumed that the ecological efficiency should be guaranteed for 300 days per year, namely between the discharges Q_{30} and Q_{330} (= discharge that is statistically not exceeded over 30 and 330 days per year, respectively). Both design criteria are of equal importance.

Methods

Experimental Setup

The tests presented herein were conducted in a rectangular tilting flume, 13.50 m long, 0.60 m wide, and 0.60 m deep, its sidewalls were made of glass and PVC to minimize wall effects (Fig. 5). The inflow section was approximately 2 m long, a flow straightener assured uniform water depth and homogeneous flow velocity in the inflow cross section. At the outflow section the bed level was fixed with a PVC plate. Erosion on the ramp followed a rotational movement around this fix point. Hence, the lower boundary condition for the bed level was constant. Uniform flow depth at the outflow section was closely achieved with an adjustable needle weir. The transported sediment was caught in a filtering basket submerged in a tank with constant water level at the outflow section.

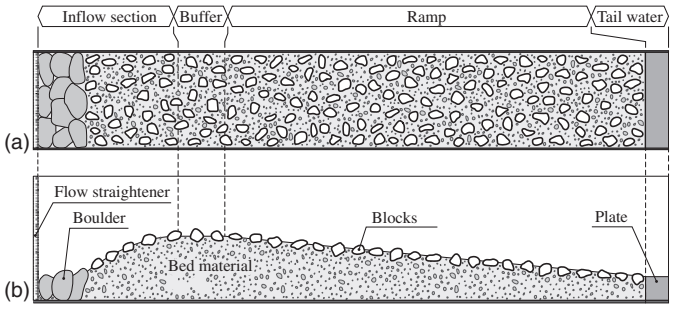

Fig. 5. (a) Plan view; (b) longitudinal section of a UBR with a 2-m-long inflow section, 1-m-long buffer area, 9-m-long ramp, and fixed tail water plate (drawing not to scale)

The flume was equipped with two pumps, delivering a maximum discharge of $Q_{\max,1} = 20$ L/s and $Q_{\max,2} = 100$ L/s, respectively. The discharge was measured by a magnetic-inductive flowmeter (MID). Some of the experiments were performed with sediment input at the inflow section. For this purpose a sediment feeder was placed above the inflow section, delivering the designed sediment supply approximately 3 m upstream of the ramp head. Locally, the water level was continuously measured with four pairs of ultrasonic sensors positioned at 1, 4, and 7 m downstream of the ramp head, respectively, as well as just before the needle weir above the fixed PVC plate. The bulk velocity U was measured with the salt dilution method (e.g., Weichert 2006; Recking et al. 2008). The mean flow velocity between the blocks is slightly higher due to the volume covered by the blocks. Salty water was injected instantaneously over the entire flume width, approximately 1 m upstream of the ramp head. The water conductivity was measured at three cross-sections ($\Delta x = 3$ m, each) with three pairs of electrodes consisting of metal bands attached to the sidewalls. U was determined by calculating the time-lag between the center of mass of the salt wave of two different cross sections (e.g., Smart and Jäggi 1983). The bed topography was determined with a laser distance sensor, mounted together with an additional ultrasonic sensor on a two-dimensional (2D) traversing system. To check local flow conditions, a point gauge was used in combination with a hydrometric vane. Three weighing cells were installed at the filtering basket to weigh the washed out sediment. The experiments were continuously observed with a fixed camera placed on the laboratory ceiling. During each run, photos were taken every 20 minutes to record the movement of the single blocks.

Requena (2008) defined two different grain size distributions: (1) a fine mixture (FM), and (2) a coarse mixture (CM) to represent the bed material of typical Swiss rivers. The FM corresponds to lower bed slopes with $0.2 < S < 0.8\%$ and CM to steep reaches with $1 < S < 1.5\%$. For the present research these mixtures were downscaled with a geometrical scale between 20 and 30 compared to a typical Swiss prealpine river reach. The characteristic parameters of FM and CM are summarized in Table 1. Both grain size distributions are considered as wide, with $\sigma = (d_{84}/d_{16})^{0.5} = 2.7$ and 3.3, respectively, so that an armoring layer may develop (Little and Mayer 1972). The sediment mixtures were prepared with natural sand or gravel material, with a density of $\rho_s \approx 2{,}650$ kg/m^3 and a minimum grain size of $d_{\min} = 0.25$ mm, to avoid cohesive effects.

Table 1. Characteristic Parameters of the Sediment Materials Used

Sediment material	d_m (mm)	d_{10} (mm)	d_{16} (mm)	d_{60} (mm)	d_{84} (mm)	d_{90} (mm)	σ
FM	1.5	0.3	0.4	1.5	2.9	3.5	2.7
UFM	3.1	2.6	2.7	3.2	3.3	3.5	1.1
CM	4.3	0.5	0.7	5	7.7	8.8	3.3
UCM	8.5	6.7	6.9	8.4	9.5	9.8	1.2

Table 2. Investigated Parameter Combinations of Each Experiment

Experiment	D (mm)	Sediment	d_{90} (mm)	D/d_{90}	λ	q [L (s · m)]	Q_s (g/s)	Number of runs
A1	43	FM	3.5	12.3	0.15	3.3–60	0	6
$A1_{rep}$	43	FM	3.5	12.3	0.15	3.3–60	0	6
A3	43	UFM	3.5	12.3	0.15	3.3–60	0	6
A5	43	FM	3.5	12.3	0.25	3.3–60	0	6
A6	65	FM	3.5	18.6	0.15	3.3–40	0	5
A7	65	FM	3.5	18.6	0.25	3.3–60	0	6
A8	43	CM	8.8	4.9	0.15	3.3–27	0	4
A9	43	CM	8.8	4.9	0.25	3.3–40	0	5
A10	65	CM	8.8	7.4	0.15	3.3–140	0	12
A11	65	CM	8.8	7.4	0.15	3.3–140	10–363	9
A12	57	CM	8.8	6.5	0.15	3.3–140	0	11
A13	65	CM	8.8	7.4	0.25	3.3–140	0	11
A14	65	CM	8.8	7.4	0.25	3.3–140	10–363	8
A15	65	UCM	9.3	7	0.15	3.3–140	0	10

Note: Every experiment (A1–A15) includes 6–12 runs with increasing q; the initial ramp slope was kept constant with $S_0 = 5\%$, so that the ramp length $L_R = 9$ m.

Additionally, two sediment mixtures with uniform grain size [uniform fine material (UFM) and uniform coarse material (UCM)] were used to investigate the influence of the standard deviation σ on the ramp stability (Table 1). Due to the armoring characteristics of the two sediment mixtures FM and CM, the sediment entrainment is dominated by the armoring layer and therefore strongly related to d_{90}. For this reason, the uniform materials were chosen to have a mean diameter d_m close to the related d_{90} of the corresponding mixture.

The characteristic grain sizes of the blocks correspond to the equivalent spherical block diameter D, defined as the diameter of a sphere of equivalent volume or mass as the considered block. The used blocks were angular natural limestones, which were ideally approximated as ellipsoids and characterized through the three axes a, b, and c. Three different block categories were used for the experiments. By sampling the weight, volume and the three axes of approximately 70–100 blocks in each category the equivalent spherical block diameters were determined to $D_1 = 43$ mm, $D_2 = 57$ mm, and $D_3 = 65$ mm.

Experimental Program and Procedure

The experimental procedure described below was kept the same for each experiment. Each experiment (A1, A2, A3, ..., Table 2) corresponds to a certain parameter combination and is subdivided into 6–12 single runs. Each run represents a constant specific discharge q ranging from 3.3 to 140 L/(s · m). A2 and A4 are not further treated in this paper because they represent different boundary conditions (Tamagni 2013). The ramp was built with a length of $L_R = 9$ m, with one of the above described bed materials (FM, CM, UFM, or UCM) with an initial slope of $S_0 = 5\%$, and was then covered with blocks of a certain D with a certain block placement density λ (Fig. 4). Experiments were formed with $\lambda = 0.15$ and 0.25. For each combination of D and λ a 1-m template was produced in plywood, where the position of each single block was cut out so that it could be reproduced to achieve similar initial conditions. The blocks were placed on the bed such that the longest axis (a-axis) was parallel to the bed. Bed material was added again so that the initial block protrusion was about $P \approx 0.5D$. A buffer area was added upstream of the ramp with a length of 1 m, a slope of 1% and covered with the same blocks and the same block placement density as along the ramp (Fig. 5). The basic idea of the buffer area is to provide stable conditions at the ramp head, even if the ramp slope becomes smaller due to erosion. During rotational erosion of the ramp around the lower fixed point the buffer area becomes a regular part of the ramp without destabilizing the ramp head. The approximately 2-m-long inflow section was covered with larger blocks on the flume bed. The funnel shape of the inflow section assured the development of turbulent channel flow and a smooth transition between inflow section and buffer area.

Before starting an experiment and after the equilibrium ramp slope S_e had been reached the ramp topography was scanned with a laser distance meter with a spatial resolution of 10×2 cm^2 in longitudinal and transverse directions. A central section of the ramp of 1 m in length was scanned with higher resolution of 1×1 cm^2. The first run with the lowest specific discharge [$q = 3.3$ L/(s · m)] was then started. The discharge was kept constant during each run until S_e was achieved. The bulk velocity, the local velocities and the local water levels were measured after equilibrium conditions had been reached. The next run started then with a higher constant q. The discharge was increased stepwise in each run until S_e was close to zero. Experiments A8 and A9 were stopped because large amounts of blocks were entrained leading to a significant reduction of λ, which is defined as a ramp failure. Either a bed slope close to zero or strongly reduced λ defined the end of an experiment.

Table 2 gives an overview of all conducted experiments including the most important parameters. All experiments were carried out under stepwise steady conditions. Constant sediment supply was given during A11 and A14 corresponding to the Meyer-Peter and Müller (1948) transport capacity assuming a bed slope of 1% representing typical prealpine conditions. Previous tests at the VAW showed that the effect of S_0 on the final equilibrium slope S_e is negligible. For this reason, the initial ramp slope S_0 was kept constant for all experiments on a steep level for UBR with $S_0 = 5\%$.

An important aspect is the definition of the equilibrium slope at the end of an experimental run. When is it reached and when to stop the experiment? The basic consideration is that the ramp reaches its equilibrium condition when the sediment input equals the sediment output. For experiments without sediment supply this condition is ideally given when no sediment is entrained and no sediment reaches the sediment basket at the end of the flume so that the weighing cells measure a constant value. In practice it may take weeks until full equilibrium is reached. A compromise between experimental duration and acceptable deviation from equilibrium needs to be found. Based on preliminary tests equilibrium conditions were assumed to be reached when the average increase of the weighed sediment was below 1.26 kg/h for at least three consecutive hours, corresponding to a change in bed slope of less than 0.001% per h. In the experiments with sediment input at the inflow section, another criterion was applied. This is necessary because close to the equilibrium condition the eroded sediment mass from the ramp is much smaller than the input mass at the inflow section, making an accurate determination of the eroded mass impossible. In this case the experiment was stopped when the difference

Fig. 6. Experiment A10 (Table 2) taken after different runs, showing the partial movement of the blocks forming more structured pattern during large discharges

between the last three hourly averaged water levels measured with ultrasonic sensors at four cross sections was smaller than 1% of the measured value. The time needed to reach equilibrium conditions for a single run varied between 3 and 100 h. The experiments with uniform material (e.g., A15 in Table 2) needed much longer runs to reach equilibrium conditions than those with sediment mixtures.

Results and Discussion

General Behavior

In general the behavior of the different ramps was quite similar. Entrainment of the bed material could be observed in particular at the beginning of each run, when equilibrium conditions were not yet reached. Over time the entrainment process of the base material led to a continuous decrease of the ramp slope. By increasing the discharge the block arrangement and the bed topography also changed. Fig. 6 shows the evolution of an UBR during Experiment A10 after achieving equilibrium conditions for different specific discharges (note that the viewing angle is not exactly the same in all the subfigures). For q up to 13 $\mathrm{L}/(\mathrm{s}\cdot\mathrm{m})$ representing a discharge below a bed forming flood event, only very local block movements can be observed with travel distances below 0.5 times the block diameter. For higher discharges up to flood events with a return period of about 100 years, the local changes are more distinct. More blocks moved up to approximately 2–3 times the block diameter, forming a more structured configuration. The authors hypothesize that the ramp adjusts itself to the higher discharge not only by flattening but also by rearranging the blocks in a more stable or more dissipative pattern. During other experiments

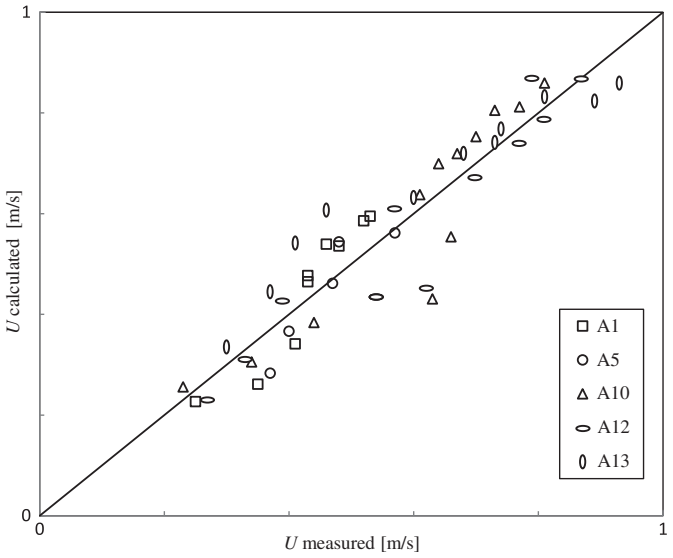

Fig. 7. Comparison between measured $U_{\_measured}$ and $U_{\_calculated}$ with Eq. (3) adapted from Pagliara and Chiavaccini (2006), where the parameter d_{84} is replaced by the protrusion of the blocks P

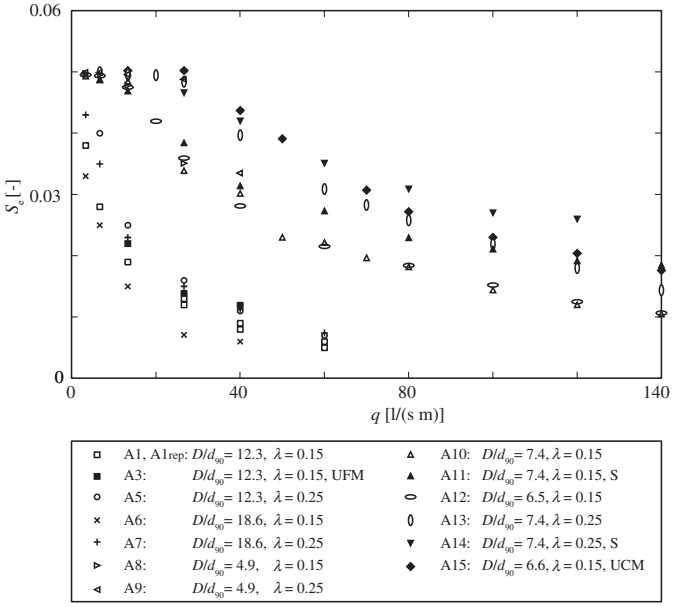

Fig. 8. Equilibrium slope S_e versus specific discharge q of every run during Experiments A1–A15

(A8 and A9) with small D/d_{90}, the blocks moved not only locally, but were transported along the ramp leading to complete failure.

Flow Resistance

The given relation for flow resistance by Pagliara and Chiavaccini (2006) [Eq. (1)] for riverbeds with macroroughness elements is based on laboratory experiments where hemispheres or crushed blocks were placed on a fixed bed. To test Eq. (1) with the present experiments, the mean flow depth h, the bulk velocity U and the shear flow velocity u^* have to be determined. The bulk velocity U was determined with the salt dilution method described in experimental setup section. The mean water depth h was determined with the continuity equation taking into account the area covered by blocks, i.e., h is the water depth between the blocks. The bulk shear velocity u_b^* is defined as $u_b^* = (ghS_e)^{0.5}$.

It turned out that Eq. (1) with $c = -2.4$ representing random disposition and crushed surface (Pagliara and Chiavaccini 2006), in general underestimates the flow resistance measured in the present study and overestimates the bulk flow velocity U. The reason for that can be found in the parameterization of the bed roughness with the characteristic grain size d_{84} of the bed material and in the definition of the water depth in their study. By keeping the structure of Eq. (1) and replacing d_{84} with the protrusion P which in the present study was on average about 74% of the block diameter at the end of the experiments, and by further adapting the coefficients, the following equation was found:

$$\frac{U}{u_{*,b}} = 1.9(1+\lambda)^{-0.5} S^{-0.21} \left(\frac{h}{P}\right)^{0.29} \tag{3}$$

Fig. 7 compares the flow resistance expressed as the ratio between bulk velocity U, resulting from the experiments ($U_{\_measured}$) and determined with Eq. (3) ($U_{\_calculated}$). In general, the trend of the present data is well represented ($R^2 = 0.87$), it is assumed that this equation is valid for UBR with similar ranges of D/d_{90} and λ, with movable bed and movable blocks including a quite heterogeneous geometry.

Ramp Stability

The experiments were performed under stepwise increasing steady discharge conditions (Tamagni 2013). Each step represents the peak discharge of a certain flood event. The discharge increment was chosen such that the armor layer from the previous run completely broke up. The developed bed slope represents the minimum possible slope in function of a certain specific discharge [$S_e = f(q)$] due to the long test duration and the harsh criterion to reach equilibrium conditions, which are rarely reached under prototype conditions. Therefore, the resulting stability curves $S_e = f(q)$ represent a conservative assumption for the ramp design, covering a certain range of uncertainties associated with natural irregular block shape and diameter and natural variability in the bed material. Fig. 8 shows a stability diagram, namely the relationship between q and S_e, for all experiments.

To parameterize the resulting equilibrium slope S_e the following parameters were considered: specific discharge q, equivalent spherical block diameter D, the ratio between block diameter and characteristic grain size D/d_{90}, block placement density λ, the gravity acceleration g and the ratio between sediment and water density $s = \rho_s/\rho = 2.65$, so that $S_e = f(q, D, D/d_{90}, \lambda, g, s)$. To find a suitable relation describing S_e, the effect of these parameters was analyzed and introduced stepwise as follows.

Effect of Block Diameter

The comparison of Experiment A2 without blocks with the other experiments with blocks of different size allows for some considerations about the influence of D on the ramp stability. In general, the stabilizing effect of the blocks decreases with increasing water depth h. For low relative submergences h/P, where the blocks protrude ($h < P$) or are just overflown ($h \approx P$), the form drag plays a decisive role for the flow resistance together with the grain friction. Each single roughness element (block) induces energy dissipation due to flow separation, resulting in a higher flow resistance compared to the bed without blocks, where only the grain friction of the sediment material plays a role. With increasing submergence of the blocks or h/P, respectively, the flow separation occurring at each

block decreases in relation to the overall energy dissipation. The relative roughness of the bed is lower and the form drag is less pronounced compared with low h/P values, meaning that the stabilizing effect of the blocks is most dominant for low submergence levels. This effect is visible with decreasing surface waves and vanishing local hydraulic jumps with increasing submergence levels. The effect of the block diameter D was introduced by normalizing the specific discharge by $q/[g(s-1)D^3]^{0.5}$ known as a nondimensional flow rate (e.g., Aberle and Smart 2003).

Effect of Block Placement Density

According to Rouse (1965) an optimal placement density in terms of flow resistance is between 10 and 40%, depending on the roughness shape and arrangement. Rouse (1965) suggested an optimal spherical block placement density of $\lambda_{opt} \approx 0.26$. For lower λ the maximum relative roughness and the maximum form drag, respectively, are not achieved. For higher λ, the roughness elements are too close to each other: the area affected by a single block is *disturbed* by the presence of the next block and the flow separation cannot develop completely, leading to reduced energy dissipation compared to lower λ. For λ_{opt} each single block contributes with its maximum form drag to the flow resistance. The present experiments support this finding, although no experiments were performed with λ larger than 0.25. The aim of the present research was to find an optimal parameter combination in terms of ramp stability on the one hand, but also in terms of project feasibility (e.g., cost effectiveness) on the other hand, limiting the maximal block placement density investigated to $\lambda = 0.25$.

Depending on the D/d_{90} values, the higher block placement density of $\lambda = 0.25$ led to a 10–40% increase of the equilibrium slope S_e compared to experiments with $\lambda = 0.15$. The effect of λ was included by dividing the above defined dimensionless specific discharge by λ.

Effect of D/d_{90}

As explained in the section "Stability and Design Requirements of UBR," D/d_{90} in bimodal mixtures needs to be in a certain range ($6 < D/d_{90} < 17$). If $D/d_{90} < 6$ the blocks tend to suddenly move above the bed material leading to an abrupt failure when a certain critical discharge is reached. If $D/d_{90} > 17$ the blocks tend to sink into the layer of bed material so that the dissipative properties get lost, leading to larger flow velocities with increased bed erosion. In the experiments the ramps with $D/d_{90} = 18.6$ are the least stable UBR tested, confirming the theory of Raudkivi and Ettema (1982). Through the embedding process the block protrusion P decreases with the increase of q, leading to a low final equilibrium bed slope. Experiments with $D/d_{90} = 4.9$ also confirmed the theory of Raudkivi and Ettema (1982): up to a certain q the ramp remained very stable. By further increasing q the blocks suddenly started to move and were transported along the ramp. This sudden reduction of λ led to an unfavorable sudden failure of the ramp. The transition from stable to unstable conditions happened during a short time period, precluding the adjusting process to the higher discharge with a lower bed slope similar to the failure mechanism of classical block ramps, where the failure of one local block may immediately lead to the failure of the complete structure.

In the case of $D/d_{90} = 7.4$ (A10 and A13) with different λ, the ramp remained stable also for high discharges [$q = 140$ L/(s · m)] corresponding to 100-year or even larger floods in a typical Swiss river. The bed slope did not flatten below 1%. Neither dominant block embedding, nor dominant block overpassing was observed. By varying slightly D/d_{90} to 6.5, no significant differences in terms

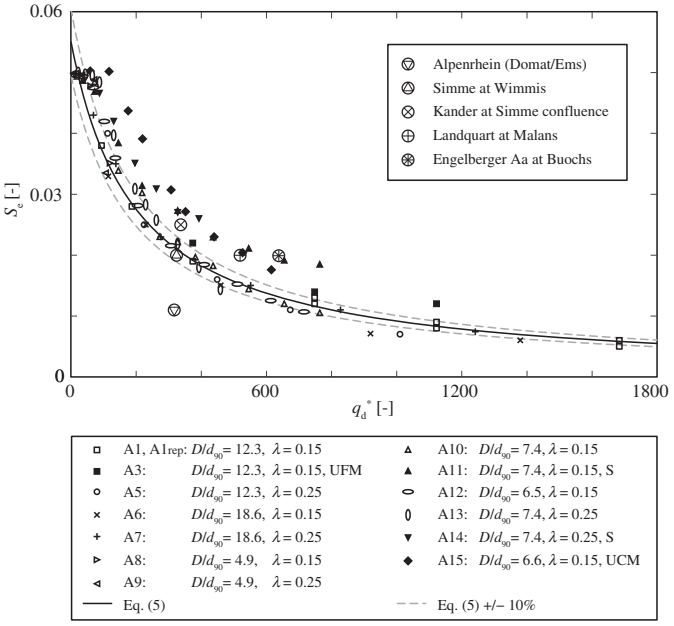

Fig. 9. Ramp stability for all conducted experiments with equilibrium slope S_e versus dimensionless specific discharge q_d^* defined in Eq. (4) [black line = Eq. (5); dotted grey lines: variation range of $+/-10\%$ with respect to Eq. (5); particularly stable experiments (A3, A11, A14, and A15) were not considered in Eq. (5); large round symbols describe prototype examples where S_e indicates the initial bed slope after construction]

of ramp stability were observed. It is concluded that the best ratio D/d_{90} in terms of ramp stability and no abrupt failure mechanism is in the range of $6.5 \le D/d_{90} \le 7.4$. Similar ramp behavior for $D/d_{90} = 6.5$ and 7.4 confirms the validity of the results. A gradual and slow erosion process by increasing q was reached, so that the uncertainties related to a characteristic grain size of the sediment material or block diameter in prototype conditions become less influential. For D/d_{90} smaller than 6.4 the failure mechanism tends towards abrupt ramp failure as shown in A8 and A9 with $D/d_{90} = 4.9$.

The effect of D/d_{90} was included in the parameterization with a power of 2 leading finally to a dimensionless discharge q_d^* of (Tamagni 2013)

$$q_d^* = \frac{q}{\sqrt{g(s-1)D^3}} \lambda^{-1} \left(\frac{D}{d_{90}}\right)^2 \tag{4}$$

The dimensionless specific discharge q_d^* is directly linked to the equilibrium slope S_e resulting from the experimental results and can be considered as design parameter for UBR. Normalized with q_d^* the data points in Fig. 8 collapse (Fig. 9). Experimental data from runs with sediment supply (A11 and A14, see section below) as well as with uniform material (A3 and A15) follow the trend as well, with slightly larger equilibrium slopes. In order to find a conservative model for design purposes, A3, A11, A14, and A15 were not considered in the following data fit (see also "Effect of Sediment Supply" section). Fig. 9 shows S_e versus q_d^* for all experiments. The black line represents the data fit for all experiments considered [Eq. (5)], describing the determined points with a coefficient of determination of $R^2 = 0.94$

$$S_e = \frac{11}{q_d^* + 200} \quad \text{for } q_d^* < 1{,}700 \tag{5}$$

Effect of Sediment Supply

To quantify the influence of incoming bed load on the ramp stability experiments were performed with sediment input at the upstream boundary. The input rate was chosen to correspond to the transport capacity of an assumed bed slope of 1% upstream of the ramp. The resulting supply rate was e.g., 45 g/s for $q = 40$ L/(s · m), 236 g/s for $q = 100$ L/(s · m), and 360 g/s for $q = 140$ L/(s · m). Considering the time t_{eq} needed to reach equilibrium conditions of these three runs a total sediment mass of 3.6, 11.9, and 9.1 t, respectively, was supplied. To reduce the experimental effort, the effect of the sediment supply was only tested on the ramp with optimal parameter combination in terms of stability, namely for $D/d_{90} = 7.4$ with $\lambda = 0.15$ (A11) and $\lambda = 0.25$ (A14), respectively.

It turned out that the sediment supply had a stabilizing effect. For $q > 40$ L/(s · m) the equilibrium slopes S_e of A11 and A14 resulted about 15 to 75% steeper than in the case without sediment supply (A10 and A13). Therefore, the authors consider the experiments without sediment supply as critical load cases and as representative for the design. The reason for the enhanced stability for runs with sediment input is the less pronounced scouring around the blocks. The transported sediment fills the scour holes leading to a better embedding and reduced movements of the blocks.

Comparison with Data of Existing UBR in Switzerland

To relate the present experimental results with UBR under prototype conditions Fig. 9 also shows some realized examples in Switzerland. The dimensionless discharge q_d^* was determined with Eq. (4) with q representing a 100-year flood event and considering the local geometrical conditions. In these cases S_e describes the initial slope after construction and not the final equilibrium slope after some flood events, as it is the case for the experimental data.

Considering the suggested Eq. (5) for the determination of S_e versus q_d^*, it is expected that the mean bed slope will further be reduced during a 100-year flood event in three cases (Kander, Landquart, and Engelberger Aa, Fig. 9). In the other two cases (Simme River and Alpine Rhine) the mean bed slope should remain stable for a 100-year flood.

Conclusions

Laboratory experiments were conducted under steady conditions for different parameter combinations to investigate the stability of unstructured block ramps. Two sediment mixtures representing typical sediment materials of Swiss Rivers and three block diameters were combined in different ways to test the effect of the bimodal mixture ratio D/d_{90}. In terms of ramp stability an optimal ratio for $6.5 < D/d_{90} < 7.4$ has been determined. Two different block placement densities λ were tested and their effect quantified: in the optimal range of D/d_{90} a block placement density $\lambda = 0.25$ has a significant stabilizing effect on the ramp, resulting in an equilibrium slope of 30–50% steeper than for $\lambda = 0.15$. Furthermore, it was shown that the experiments with uniform sediment material corresponding to d_{90} of the bed material overestimate the ramp stability. The experiments conducted with sediment supply indicated a stabilizing effect on UBR, leading to at least 10% steeper equilibrium slopes even for the largest discharges. This suggests that the experiments conducted without sediment supply represent the lower limit in terms of stability and can therefore be considered as representative for a conservative design. From these considerations a model for the determination of the ramp stability has been developed. This model allows to predict an equilibrium slope on an UBR in relation to a dimensionless discharge. In addition, the experimental data are compared with the flow resistance equation proposed by Pagliara and Chiavaccini (2006) for block ramps reinforced with boulders and suggested in the design manual of DWA (2009). Their approach generally overestimates the flow velocity on the tested UBR, due to the relative submergence defined without taking into account the protruding part of the blocks. When adapting the suggested equation from Pagliara and Chiavaccini (2006) by introducing the protrusion of the single blocks into the flow field the data can be well represented.

Acknowledgments

The project was partly funded by the Swiss Federal Office for the Environment (FOEN). Dr. Gian Reto Bezzola is gratefully acknowledged for his valuable input.

Notation

The following symbols are used in this paper:

- D = equivalent spherical block diameter (m);
- d_i = grain diameter at which i% of the sediment sample is finer than (m) or (mm);
- F = Froude number;
- g = gravity acceleration (m/s^2);
- HQ_{100} = discharge with a statistical return period of 100 years (m^3/s);
- h = mean flow depth (m);
- h/P = relative submergence;
- P = mean block protrusion;
- Q_i = discharge which statistically does not exceed i days per year (m^3/s);
- q = specific discharge (m^2/s) or [L/(s · m)];
- R = Reynolds number;
- S = ramp slope;
- S_e = equilibrium ramp slope;
- S_o = initial ramp slope;
- U = bulk velocity (m/s);
- u_* = shear velocity (m/s);
- ν = kinematic fluid viscosity (m^2/s);
- W = river width (m);
- λ = block placement density;
- ρ = water density (kg/m^3);
- ρ_s = sediment density (kg/m^3); and
- σ = standard deviation of bed material.

References

Aberle, J., and Smart, G. (2003). "The influence of roughness structure on flow resistance on steep slopes." *J. Hydraul. Res.*, 41(3), 259–269.

Alp, M., Karpati, T., Werth, S., Gostner, W., Scheidegger, C., and Peter, A. (2011). "Erhaltung und Förderung der Biodiversität von Fliessgewässern [Preservation and valorization of the biodiversity in rivers]." *Wasser Energie Luft*, 103(3), 216–223 (in German).

Bezzola, G. R., and Hegg, C. (2008). "Ereignisanalyse Hochwasser 2005, Teil 2—Analyse von Prozessen, Massnahmen und Gefahrengrundlagen [Analysis of flood event 2005. Part 2: Analysis of processes, measures and fundamentals of risks]." *Umwelt-Wissen Nr. 0825*, Bundesamt für Umwelt BAFU, Eidgenössische Forschungsanstalt WLS, Bern, Switzerland (in German).